

## Imprint of PBH domination on gravitational waves generated by cosmic strings

Debasish Borah<sup>1,\*</sup>, Suruj Jyoti Das<sup>1,†</sup>, Rishav Roshan<sup>2,3,‡</sup> and Rome Samanta<sup>4,§</sup>

<sup>1</sup>*Department of Physics, Indian Institute of Technology Guwahati, Assam 781039, India*

<sup>2</sup>*Department of Physics, Kyungpook National University, Daegu 41566, Korea*

<sup>3</sup>*Center for Precision Neutrino Research, Chonnam National University, Gwangju 61186, Korea*

<sup>4</sup>*CEICO, Institute of Physics of the Czech Academy of Sciences, Na Slovance 1999/2, 182 21 Prague 8, Czech Republic*



(Received 9 May 2023; accepted 6 July 2023; published 31 July 2023)

We study the effect of an ultralight primordial black hole (PBH) dominated phase on the gravitational wave (GW) spectrum generated by a cosmic string (CS) network formed as a result of a high-scale  $U(1)$  symmetry breaking. A PBH-dominated phase leads to tilts in the spectrum via entropy dilution and generates a new GW spectrum from PBH density fluctuations, detectable at ongoing and planned near-future GW detectors. The combined spectrum has a unique shape with a plateau, a sharp tilted peak over the plateau, and a characteristic falloff, which can be distinguished from the one generated in the combination of CS and any other matter domination or new exotic physics. We discuss how ongoing and planned future experiments can probe such a unique spectrum for different values of  $U(1)$  breaking scale and PBH parameters such as initial mass and energy fraction.

DOI: [10.1103/PhysRevD.108.023531](https://doi.org/10.1103/PhysRevD.108.023531)

### I. INTRODUCTION

While the standard model (SM) of particle physics has been the most successful phenomenological model explaining the elementary particles and their interactions except gravity, it cannot explain several observed phenomena like neutrino mass, dark matter (DM), and baryon asymmetry. This has motivated the pursuit of exploring beyond standard model (BSM) scenarios for several decades. However, none of the particle physics-based experiments, including the ongoing Large Hadron Collider (LHC), have seen any signatures of BSM physics to date. This has garnered significant late interest in exploring alternative BSM-search strategies. Interestingly, the onset of the direct discovery of gravitational waves (GW) by the LIGO-VIRGO collaboration [1] has opened up an entirely new frontier to search for BSM physics with primordial gravitational waves. For example, BSM physics related to

inflation, first-order phase transition, topological defects, and primordial black holes (PBHs) may produce stochastic GW background within experimental sensitivity of ongoing and future planned experiments. This offers a synergic probe of BSM physics and could be the only realistic probe in some scenarios that are out of reach of particle physics experiments in the foreseeable future. See a recent review [2] discussing GW signatures of BSM physics.

Many well-motivated BSM scenarios lead to the formation of topological defects like cosmic strings and domain walls [3]. In particular, Abelian gauge extensions of the SM, with several particle physics motivations [4], lead to the formation of cosmic strings (CSs) after spontaneous symmetry breaking [5,6]. These CSs can generate stochastic GW background with a characteristic spectrum which can be observed at near future GW detectors if the symmetry breaking scale is sufficiently high [7,8], far outside the reach of the direct probe at experiments like the LHC. After the recent findings by the NANOGrav collaboration suggesting a stochastic common spectrum process across many pulsars [9], CSs as a source of primordial GWs gained a great deal of attention [10–14]. While a scale-invariant GW spectrum at higher frequencies is a typical signature of CSs, any deviation from this spectrum can signify additional new physics or nonstandard cosmological epochs in the early universe. For example, early matter domination (EMD) can lead to spectral breaks in the CS-generated GW spectrum [15–17]. Such an EMD phase can arise due to

\*[dborah@iitg.ac.in](mailto:dborah@iitg.ac.in)

†[suruj@iitg.ac.in](mailto:suruj@iitg.ac.in)

‡[rishav.roshan@gmail.com](mailto:rishav.roshan@gmail.com)

§[samanta@fzu.cz](mailto:samanta@fzu.cz)

Published by the American Physical Society under the terms of the [Creative Commons Attribution 4.0 International license](https://creativecommons.org/licenses/by/4.0/). Further distribution of this work must maintain attribution to the author(s) and the published article's title, journal citation, and DOI. Funded by SCOAP<sup>3</sup>.

long-lived particle [18,19], PBH, or a combination of both [20,21]. Similarly, new physics, which might incorporate an additional source of GWs, can also lead to distortions in the CS-generated GW spectrum. For instance, a first-order phase transition (FOPT) induced GW together with the CS generated GW spectrum [22,23] can have distinct features which can be detectable at near future experiments if the FOPT is a supercooled one [23]. While the effect of EMD due to PBHs on CS-generated GW spectrum has been studied in several works [21,24–27], not much attention has been paid to the additional effect caused by GWs originating from PBHs themselves except for [26], where the individual GW contributions from CSs and PBHs were studied in the context of superheavy dark matter and high scale leptogenesis.

Motivated by these, we perform a general study on the effect of an ultralight PBH-dominated epoch on the CS-generated GWs and present the result for the combined spectrum that also includes, unlike any other EMDs, features of GWs caused by PBHs themselves. Among the various ways PBHs associate with GWs, we consider the one induced due to PBH density fluctuations [28–33]. For ultralight PBH domination, this GW contribution remains detectable in ongoing and near-future experiments. We show that the combined spectrum exhibits a plateau, a red tilt followed or preceded by a sharp blue tilt. Besides being distinct from any other spectrum, e.g., a CS-generated GW spectrum with an EMD caused by a fermion/scalar field [19,34,35], the overall spectrum offers characteristic features that can be detected either with a single detector or with multiple detectors in a complementary way.

This paper is organized as follows. In Secs. II and III, we briefly summarize the GW production from cosmic strings and PBH density fluctuations, respectively. In Sec. IV, we discuss the combined GW spectrum and finally conclude in Sec. V.

## II. GRAVITATIONAL WAVES FROM COSMIC STRINGS

If the vacuum manifold of a symmetry group after spontaneous symmetry breaking is not simply connected, one-dimensional topological defects namely, cosmic strings are formed [5,6]. Such a possibility naturally arises in popular  $U(1)$  extensions of the SM. If this  $U(1)$  symmetry is a gauged one, then the cosmic string loops lose their energy dominantly in the form of GW radiation, as suggested by numerical simulations based on Nambu-Goto action [36,37]. For a sufficiently high  $U(1)$  symmetry breaking scale ( $\Lambda_{\text{CS}} \gtrsim 10^9$  GeV), the resulting GW background is detectable at ongoing and near future GW experiments. This makes CS generated GW an outstanding probe of superhigh scale BSM physics [19,38–51] which cannot be probed directly at terrestrial experiments. The key parameter related to CS is their normalized tension  $G\mu \sim G\Lambda_{\text{CS}}^2$  with  $G$  being Newton's constant.

In the absence of thermal friction leading to dampening of the motion of a long-string network [52], shortly after formation, the network oscillates (at  $t_{\text{osc}}$ ) and enters the scaling regime [37,53,54] which is an attractor solution of two competing dynamics namely, the stretching of the long-string correlation length due to cosmic expansion and the fragmentation of the long strings into loops which oscillate to produce particle radiation or GWs [7,8,55].

A set of normal-mode oscillations with frequencies  $f_k = 2k/l$  constitute the total energy loss from a cosmic string loop, where the mode numbers are denoted by  $k = 1, 2, 3, \dots, \infty$ . The GW energy density parameter can, therefore, be defined as  $\Omega_{\text{GW}}(t_0, f) = \sum_k \Omega_{\text{GW}}^{(k)}(t_0, f)$ , with  $t_0$  being the present time and  $f \equiv f(t_0) = f_k a(t_0)/a(t)$ . The corresponding GW energy density at the present epoch for the mode  $k$  can be computed with the integral [56]

$$\Omega_{\text{GW}}^{(k)}(t_0, f) = \frac{2kG\mu^2\Gamma_k}{f\rho_c} \int_{t_{\text{osc}}}^{t_0} dt \left[ \frac{a(t)}{a(t_0)} \right]^5 n(t, l_k), \quad (1)$$

where  $n(t, l_k)$  is a scaling loop number density which can be computed analytically using the velocity-dependent-one-scale (VOS) [57–60] model,  $\rho_c$  is the critical energy density of the universe and  $\Gamma_k = \frac{\Gamma k^{-\delta}}{\zeta(\delta)}$  depends on the small-scale structures in the cosmic string loops such as cusps ( $\delta = 4/3$ ) and kinks ( $\delta = 5/3$ ). Here, we consider only cusps to compute the GW spectrum; a similar analysis can also be done considering kinks. While it is clear that for higher modes, contributions to the GWs from cusps are dominant, the number of cusps and kinks per loop oscillation cannot be straightforwardly determined with numerical simulations, which do not include gravitational wave backreaction in general. A preference for cusps over kinks comes from the so-called smoothing mechanism, where the kinky loops are expected to be smoothed out due to the gravitational wave backreaction [61]. This mechanism, however, has been challenged in [62,63]. Therefore, we would like to place the consideration of cusps over kinks in this article as a choice rather than a preference. The integration in Eq. (1) may be subjected to another constraint: the critical size of the loops below which particle production is dominant. This constraint corresponds to a lower bound on the time GW radiation becomes effective [64,65]. We carefully consider this constraint in the numerical analysis.

A characteristic feature of the GW spectrum generated by CS is the flat plateau due to loop formation and decay during the radiation dominated phase of the universe, with an amplitude given by

$$\Omega_{\text{GW}}^{(k=1), \text{plateau}}(f) = \frac{128\pi G\mu A_r}{9\zeta(\delta) \epsilon_r} \Omega_r [(1 + \epsilon_r)^{3/2} - 1], \quad (2)$$

where  $\epsilon_r = \alpha/\Gamma G\mu$  with  $\alpha$  the initial (at  $t = t_i$ ) loop size parameter,  $\Omega_r \simeq 9 \times 10^{-5}$  and  $A_r = 5.4$  [60]. In our work, we have considered  $\alpha \simeq 0.1$  [56,66] (as indicated by numerical simulations),  $\Gamma \simeq 50$  [55,56,66], and cosmic microwave background (CMB) constraint  $G\mu \lesssim 10^{-7}$  [67] which lead to  $\alpha \gg \Gamma G\mu$ . In this limit, Eq. (2) implies  $\Omega_{\text{GW}}^{(k=1)}(f) \sim \Lambda_{\text{CS}}$ , a property that makes models with larger symmetry breaking scales more testable with GWs from CSs. While this proportionality is robust for large loops ( $\alpha \simeq 0.1$ ), the overall magnitude of  $\Omega_{\text{GW}}^{(k=1)}(f)$  in Eq. (2) obtained from the VOS model differs from that of the numerical simulations by order of magnitude. This is related to the fact that the VOS model considers all the loops contributing to the GWs to be created with the same initial size. On the other hand, numerical simulations find only 10% of energy from the long strings going to the large loops ( $\alpha \simeq 0.1$ ), which contribute to the GWs; the rest is transferred to the smaller loops in the form of kinetic energy which redshifts away and does not contribute to the GWs [56]. Therefore, a factor  $\mathcal{F}_\alpha \simeq 0.1$  is introduced in Eq. (2) (which is equivalent to normalizing loop number density in the VOS model, where the normalization factor is  $\mathcal{F}_\alpha$ , see, e.g., Sec. V of [45] for a comprehensive description of normalization) such that the string network evolution and its properties can be described consistently with the VOS model, and at the same time, with the numerical simulations.

We shall see later in this article that in the presence of a matter-dominated epoch before the most recent radiation domination, the plateau breaks at a frequency  $f_\Delta$  and the spectrum falls as  $\Omega_{\text{GW}}(f > f_\Delta) \sim f^{-1}$  for the fundamental mode of loop oscillations. The frequency  $f_\Delta$  carries the information regarding the end of the matter domination and, potentially, other properties of the object/field associated with the matter domination.

### III. GRAVITATIONAL WAVES FROM PRIMORDIAL BLACK HOLES

Primordial black holes (a recent review can be found in [28]), originally proposed by Hawking [68,69], can have many interesting cosmological consequences [70,71] including detection prospects via GWs. While PBHs can have a wide range of masses, we are interested in the ultralight regime in which they evaporate by emitting Hawking radiation [68,69] before the Big Bang Nucleosynthesis (BBN) epoch and hence are less constrained from cosmological and astrophysical observations. In the early universe, PBHs can be formed in a variety of ways such as from inflationary perturbations [72–76], first-order phase transition [77–85], the collapse of topological defects [86,87], etc. Here we remain agnostic about such a production mechanism and assume an initial abundance of PBHs (of Schwarzschild type) with a monochromatic mass function. The PBH is assumed to be formed in the era of

radiation domination after inflation, and its abundance is characterized by a dimensionless parameter  $\beta$  defined as

$$\beta = \frac{\rho_{\text{BH}}(T_{\text{in}})}{\rho_{\text{R}}(T_{\text{in}})}, \quad (3)$$

where  $\rho_{\text{BH}}(T_{\text{in}})$  and  $\rho_{\text{R}}(T_{\text{in}})$  represent the initial PBH energy density and radiation energy density, respectively, while  $T_{\text{in}}$  denotes the temperature at the time of PBH formation. Such a PBH can lead to an early matter domination phase if its initial energy fraction  $\beta$  exceeds a critical value defined by [88]

$$\beta < \beta_c \equiv \gamma^{-1/2} \sqrt{\frac{\mathcal{G} g_{\star,H}(T_{\text{BH}})}{10640\pi}} \frac{M_{\text{pl}}}{m_{\text{in}}}, \quad (4)$$

where

$$g_{\star,H}(T_{\text{BH}}) \equiv \sum_i \omega_i g_{i,H} e^{-\frac{M_{\text{BH}}}{\beta_i M_i}}; \quad (5)$$

$$g_{i,H} = \begin{cases} 1.82 & \text{for } s = 0, \\ 1.0 & \text{for } s = 1/2, \\ 0.41 & \text{for } s = 1, \\ 0.05 & \text{for } s = 2, \end{cases}$$

with  $\omega_i = 2s_i + 1$  for massive particles of spin  $s_i$ ,  $\omega_i = 2$  for massless species with  $s_i > 0$  and  $\omega_i = 1$  for  $s_i = 0$ .  $\beta_s = 2.66, 4.53, 6.04, 9.56$  for  $s_i = 0, 1/2, 1, 2$ , respectively, whereas  $M_i = \frac{1}{8\pi G m_i}$ , where  $m_i$  is the mass of the  $i$ th species [88].  $\gamma \simeq 0.2$  denotes a numerical factor related to the uncertainty of the PBH formation,  $\mathcal{G} \sim 4$  is the gray-body factor with  $m_{\text{in}}$  and  $T_{\text{BH}}$  denoting the mass of PBH at the time of formation and instantaneous Hawking temperature of PBH, respectively.

As per GW signatures of PBHs are concerned, there are a variety of ways this can happen. The evaporation of the PBH itself can produce gravitons which might constitute an ultra-high frequency GW spectrum [89]. The PBH can also form mergers, leading to GW emission [90]. In addition, the scalar perturbations leading to the formation of the PBH can induce GWs at second order [91], which can be further enhanced during the PBH evaporation [92]. Finally, the inhomogeneity in the distribution of the PBH may also induce GWs at second order, as recently studied in Refs. [30–32]. We concentrate on this last possibility particularly because it can be tackled while being agnostic about PBH formation history, and the resulting GW spectrum can be probed at ongoing as well as planned near-future GW detectors.

The distribution of PBHs after they are formed is random and follows Poissonian statistics [30]. When PBHs dominate the universe's energy density, these inhomogeneities induce GWs at the second order, which are enhanced further during PBH evaporation [32]. The dominant

contribution to the GW amplitude observed today can be written as [26,32,93]

$$\Omega_{\text{gw}}(t_0, f) \simeq \Omega_{\text{gw}}^{\text{peak}} \left( \frac{f}{f_{\text{peak}}} \right)^{11/3} \Theta(f_{\text{peak}} - f), \quad (6)$$

where

$$\Omega_{\text{gw}}^{\text{peak}} \simeq 2 \times 10^{-6} \left( \frac{\beta}{10^{-8}} \right)^{16/3} \left( \frac{m_{\text{in}}}{10^7 \text{ g}} \right)^{34/9}. \quad (7)$$

The GW spectrum has an ultraviolet cutoff at frequencies corresponding to comoving scales representing the mean separation between PBHs [30,32], which is given by

$$f_{\text{peak}} \simeq 1.7 \times 10^3 \text{ Hz} \left( \frac{m_{\text{in}}}{10^4 \text{ g}} \right)^{-5/6}. \quad (8)$$

Although we shall use Eqs. (6)–(8) for numerical computation, we note that the amplitude of the induced GWs is sensitive to the width of the PBH mass function [92,94,95]. In addition, density perturbations can become nonlinear during the PBH-dominated era, leading to a suppression of the spectrum [95].

#### IV. THE COMBINED GW SPECTRUM, DETECTION PROSPECTS, AND REALISTIC BSM PHYSICS SCENARIOS

##### A. The combined spectrum

As mentioned earlier, ultralight PBHs with  $\beta > \beta_c$  can affect the CS-generated GW spectrum in two ways: introducing spectral break due to PBH domination plus evaporation and introducing a new GW source from density fluctuations. Because of the PBH-induced early matter domination before BBN, the plateau region of the CS-generated GW spectrum gets broken [15–17] at a turning point frequency  $f_{\Delta}$  which can be determined by the time say  $t_{\Delta}$  (or equivalently the PBH evaporation temperature  $T_{\Delta}$ ) at which the early matter domination ends and the standard radiation era begins. The frequency  $f_{\Delta}$  (present day) is equivalent to twice the inverse length  $l_M^{-1}$  of a loop (with initial size  $at_{\Delta}$ ) corresponding to the maximal emission of GWs at  $t_M > t_{\Delta}$ . A higher value of  $f_{\Delta}$  would imply the loop was produced earlier—radiation domination began earlier. A loop created at a time  $t_{\Delta}$  contributes maximally to Eq. (1) when it reaches its half-life, i.e.,  $l_M(t_M) = \frac{at_{\Delta}}{2}$  [16]. Therefore, the frequency observed today for GWs emitted at  $t_M$  is given by

$$\begin{aligned} f_{\Delta} &= \frac{4}{at_{\Delta}} \frac{a_M}{a_0} = \sqrt{\frac{8}{\alpha \Gamma G \mu}} t_{\Delta}^{-1/2} t_{\text{eq}}^{1/6} t_0^{-2/3} \\ &\simeq \sqrt{\frac{8 z_{\text{eq}}}{\alpha \Gamma G \mu}} \left( \frac{t_{\text{eq}}}{t_{\Delta}} \right)^{1/2} t_0^{-1}, \end{aligned} \quad (9)$$

where  $a_M$  is the scale factor at the time  $t_M = \frac{at_{\Delta}}{2\Gamma G \mu}$ ,  $t(z)_{\text{eq}}$  is the time (redshift  $\sim 3400$ ) corresponding to the standard matter-radiation equality, and  $t_0$  is the present time. Equation (9) can be conveniently recast in terms of PBH evaporation and present-day temperatures as

$$\begin{aligned} f_{\Delta} &= \sqrt{\frac{8}{z_{\text{eq}} \alpha \Gamma G \mu}} \left( \frac{g_*(T_{\Delta})}{g_*(T_0)} \right)^{1/4} \frac{T_{\Delta}}{T_0} t_0^{-1} \\ &\simeq 0.656 \left( \frac{\alpha}{0.1} \right)^{-1/2} \left( \frac{\Gamma}{50} \right)^{-1/2} \left( \frac{G \mu}{10^{-13}} \right)^{-1/2} \\ &\quad \times \left( \frac{g_*(T_{\Delta})}{g_*(T_0)} \right)^{1/4} \left( \frac{T_{\Delta}}{\text{GeV}} \right) \text{ Hz}, \end{aligned} \quad (10)$$

which implies, e.g., if the PBHs evaporate at  $T_{\Delta} = 1$  TeV and 1 MeV, the plateau of the GW spectrum gets broken at  $f_{\Delta} \simeq 1558$  Hz and 0.9 mHz, respectively, for typical values of  $G\mu$ ,  $\Gamma$ ,  $\alpha$  in Eq. (10). Beyond  $f_{\Delta}$ , the spectrum goes as  $\Omega_{\text{GW}} \sim f^{-1}$  for  $k = 1$  mode (when infinite modes are summed,  $\Omega_{\text{GW}} \sim f^{-1/3}$  [17,24,96,97]). This fall persists in general because, for considerably long PBH domination, contributions from the loops produced in the PBH-dominated era and before, are negligible or show up at higher frequencies with subdominant amplitude which we do not discuss in detail in this paper. Thus, the primary first effect or outcome due to the PBH domination is a flat GW spectrum turning red beyond  $f_{\Delta}$ .

When the second effect, i.e., the contribution of the GWs from PBH density fluctuation, is considered, the combined spectrum shows a blue tilted peak with a sharp cutoff at  $f_{\text{peak}}$ , in addition to the plateau and the red tilt feature discussed above. Depending on the value of  $f_{\text{peak}}$  and  $f_{\Delta}$ , we consider three distinct cases to discuss our results: (i)  $f_{\text{peak}} > f_{\Delta}$ , (ii)  $f_{\text{peak}} < f_{\Delta}$ , and (iii)  $f_{\text{peak}} \sim f_{\Delta}$ .

In Fig. 1, we show the combined spectrum corresponding to subcases (i) and (ii) for a fixed value of  $G\mu = 10^{-13}$ . The PBH parameters,  $\beta$ ,  $m_{\text{in}}$ , are chosen in such a way that the left panel plot corresponds to (i)  $f_{\text{peak}} > f_{\Delta}$  whereas the right panel shows the spectrum for (ii)  $f_{\text{peak}} < f_{\Delta}$ . Each plot uses two different PBH benchmarks to show the peak position and amplitude shift. To show the variation due to the CS parameter  $G\mu$ , we plot the combined spectrum for different values of  $G\mu$  in Fig. 2. The PBH parameters are kept fixed in both left and right panel plots of Fig. 2, whereas  $G\mu$  values are chosen in such a way that left and right panels correspond to subcases (i) and (ii), respectively. Finally, in Fig. 3, we show the subcase (iii)  $f_{\text{peak}} \sim f_{\Delta}$  for different combinations of CS and PBH parameters.<sup>1</sup> In all of these plots, the experimental sensitivities of SKA [98], GAIA [99], EPTA [100], THEIA [99],  $\mu$ ARES [101],

<sup>1</sup>Note that another interesting frequency  $f_{\text{eva}}$  corresponding to the wave number that crosses the horizon at  $T_{\Delta}$  is, in general, different from  $f_{\Delta}$  because  $f_{\text{peak}} \gg f_{\text{eva}}$  [32].

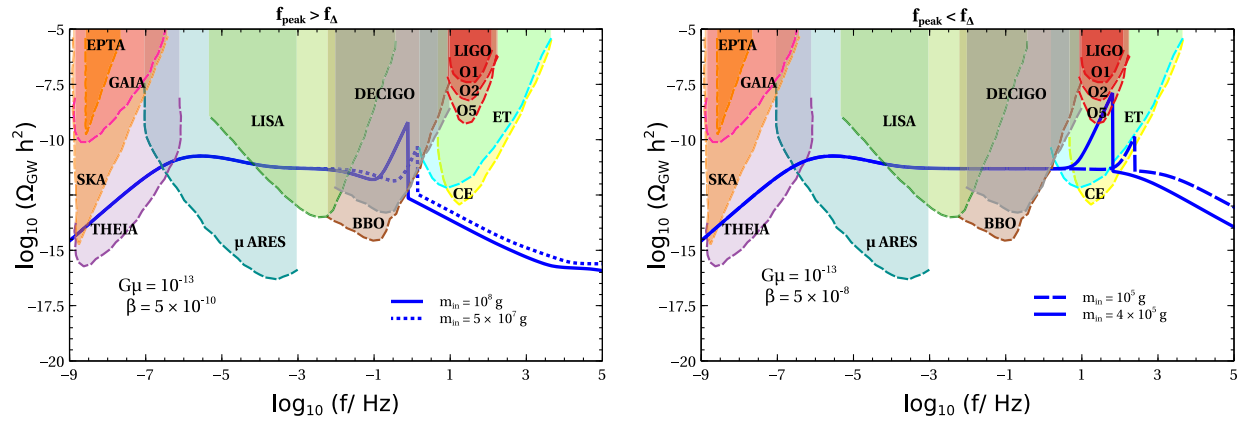


FIG. 1. Combined GW spectra from cosmic strings and PBH density fluctuations, for a fixed value of  $G\mu$  and for different values of initial PBH mass  $m_{\text{in}}$ . In the left panel, we have  $f_{\text{peak}} > f_{\Delta}$ , whereas in the right panel,  $f_{\text{peak}} < f_{\Delta}$ .

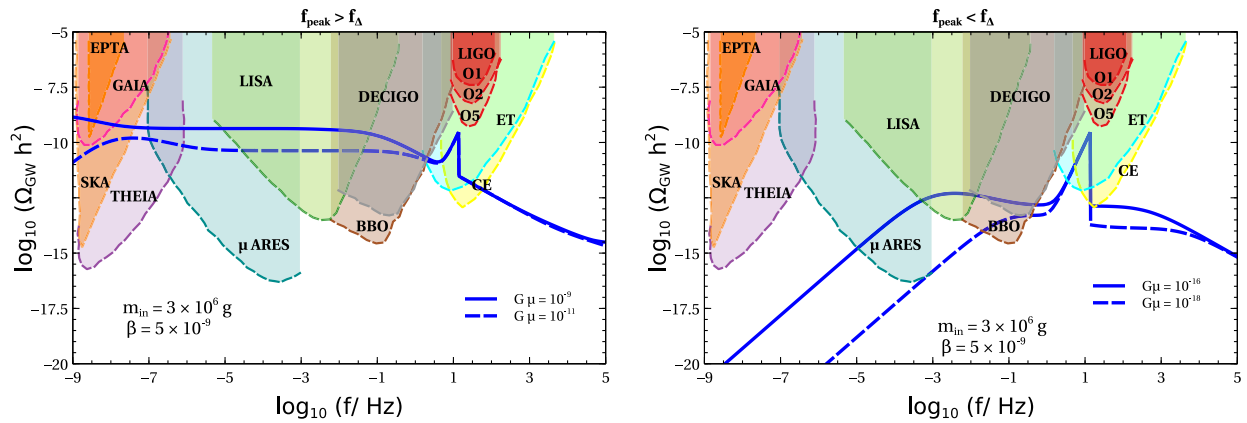


FIG. 2. Combined GW spectra from cosmic strings and PBH density fluctuations, for a fixed value of initial PBH mass  $m_{\text{in}}$ , and for different values of  $G\mu$ . In the left panel, we have  $f_{\text{peak}} > f_{\Delta}$ , whereas in the right panel,  $f_{\text{peak}} < f_{\Delta}$ .

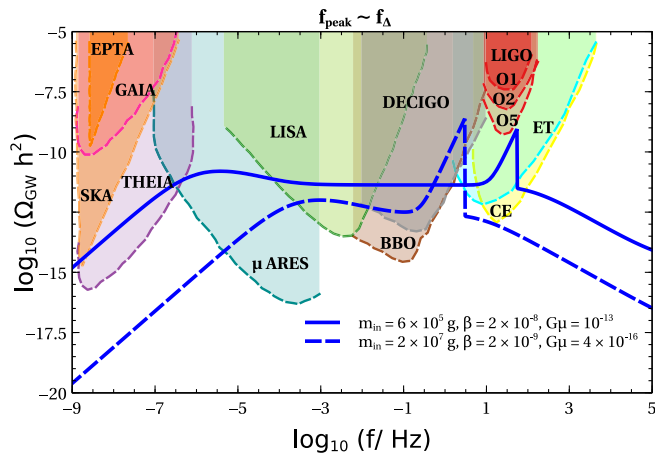


FIG. 3. Combined GW spectra from cosmic strings and PBH density fluctuations, choosing benchmark values for which  $f_{\text{peak}} \sim f_{\Delta}$ .

LISA [102], DECIGO [103], BBO [104], ET [105], CE [106], and aLIGO [107] are shown as shaded regions of different colors. Clearly, depending upon the combination of  $(G\mu, \beta, m_{\text{in}})$  different parts of the spectrum—the plateau, peak, and the turning point frequency  $f_{\Delta}$ —remain within reach of different near future GW experiments. For convenience, we present a summary table including five benchmark points (those can also be found in the figures) and list the detectors with the potential to detect such unique GW signatures. Finally, in Fig. 4 (left panel), we show the variation of  $f_{\Delta}$  with  $m_{\text{in}}$  for three different values of  $G\mu$ . In this plot, the yellow-shaded triangular region in the upper right corner corresponds to the region where particle production from the CS is more efficient than GW radiation [65]. As mentioned earlier, this constraint comes from the critical size of the loops below which particle radiation becomes dominant. It translates further to a lower bound on the initial time considered to compute the GW spectrum and introduces a break ( $f_*$ ) in the spectrum similar to the early matter domination. Requiring that

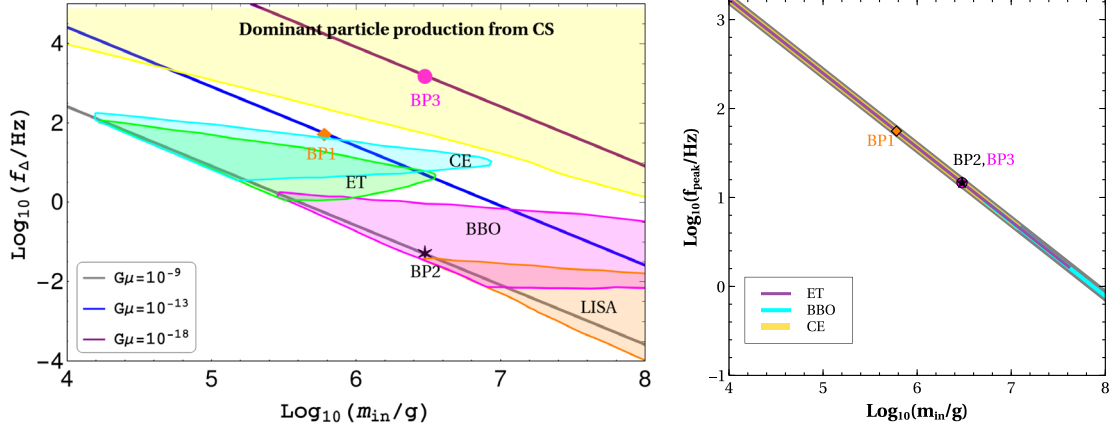


FIG. 4. Left panel: variation of  $f_{\Delta}$  with  $m_{\text{in}}$ . In the yellow-shaded region, particle production from CS is dominant over GW radiation. Right panel: variation of  $f_{\text{peak}}$  with  $m_{\text{in}}$ . In both of the plots, BP1, BP2, and BP3 (cf. Table I) are also shown with diamond, star, and circle, respectively. The sensitivities of different GW detectors are indicated too.

$f_* > f_{\Delta}$ , for the loops containing cusps-like structures, the constraint on the parameter space can be derived as [19]

$$G\mu > 2.4 \times 10^{-16} \left( \frac{T_{\Delta}}{\text{GeV}} \right)^{4/5}. \quad (11)$$

We translate this constraint to the  $f_{\Delta} - m_{\text{in}}$  plane using Eq. (10) and the evaporation temperature of PBHs in the case where they dominate [24]. In the right panel of Fig. 4, we show the variation of  $f_{\text{peak}}$  with  $m_{\text{in}}$ , which is independent of  $G\mu$ . In both of these plots, we indicate the sensitivities of different GW detectors and show three of the five benchmark points listed in Table I. As expected, in these plots, for BP1 ( $G\mu = 10^{-13}$ ) both  $f_{\Delta}$  and  $f_{\text{peak}}$  fall within CE sensitivity whereas  $f_{\text{peak}}$  lies within ET sensitivity as well. On the other hand, BP2 ( $G\mu = 10^{-9}$ ) and BP3 ( $G\mu = 10^{-18}$ ) correspond to the scenarios where  $f_{\text{peak}} > f_{\Delta}$  and  $f_{\text{peak}} < f_{\Delta}$ , respectively. The analytical estimate of the turning point frequencies matches with our numerical analysis performed in generating Figs. 1–3, up to a difference of less than  $\mathcal{O}(1)$ .

### B. A brief summary of the detection prospect

Consider that, at low frequencies, we measure the stochastic GW background from cosmic strings (e.g., the

recent finding of a stochastic common spectrum process by NANOGrav can be well explained by GWs from cosmic string for the parameter range  $G\mu \in 10^{-11} - 10^{-9}$  [10–13]). Then in Eq. (10), we have only one free parameter  $T_{\Delta}$ . In the case of PBH domination, this parameter is basically  $m_{\text{in}}$  since it appears as the only free parameter in  $T_{\Delta}$ . Therefore, if we observe a spectral break frequency  $f_{\Delta}$  at any high-frequency detector, e.g., ET and CE, we expect another sharp peak at a “predicted frequency ( $f_{\text{peak}}$ )” according to Eq. (8), or vice versa. Such a complementary detection prospect distinguishes the PBH-dominated epoch from any other EMDs. In this context, let us highlight the consequence of summing over all the modes while computing the GW spectrum from cosmic strings, especially for  $f_{\text{peak}} > f_{\Delta}$ . Because summing over large  $k$  modes changes the slope of the spectrum from  $f^{-1}$  to  $f^{-1/3}$  (loops containing cusps), such a  $f_{\Delta} - f_{\text{peak}}$  complementary detection prospect requires a longer period of PBH domination [large  $\beta$ , cf. Eq. (7)] compared to the simplest  $k = 1$  case, so that  $\Omega_{\text{gw}}^{\text{peak}}(f_{\text{peak}} > f_{\Delta}) \gg \Omega_{\text{gw}}^{\text{CS}}(f_{\text{peak}} > f_{\Delta})$ .

### C. Connection to realistic BSM scenarios

Given the general discussion above, let us point out how such a spectrum could be a probe of particle physics models. First, although the PBHs eventually evaporate,

TABLE I. Benchmark points (BP) along with the GW detectors which can detect the peak frequency  $f_{\text{peak}}$  and the turning point frequency  $f_{\Delta}$  of the combined GW spectrum.

BP	$m_{\text{in}}(g)$	$G\mu$	$\beta$	$f_{\text{peak}}$	$f_{\Delta}$
BP1	$6 \times 10^5$ g	$10^{-13}$	$2 \times 10^{-8}$	ET, CE	CE
BP2	$3 \times 10^6$ g	$10^{-9}$	$5 \times 10^{-9}$	ET, CE	BBO, DECIGO
BP3	$3 \times 10^6$ g	$10^{-18}$	$5 \times 10^{-9}$	ET, CE	None
BP4	$4 \times 10^5$ g	$10^{-13}$	$5 \times 10^{-8}$	LIGO, CE, ET	CE
BP5	$10^8$ g	$10^{-13}$	$5 \times 10^{-10}$	BBO, DECIGO	LISA, BBO, DECIGO

they might produce stable or unstable relics. A stable relic could be dark matter, whereas an unstable particle (such as right-handed neutrinos in seesaw mechanism) produced from PBHs may seed baryogenesis (see, e.g., Refs. [108–111]). In addition, depending on the mass and relative energy fraction, a PBH-dominated universe can alter the standard parameter space of many high-energy models, e.g., dark matter models [112], and the models of light QCD axions [113]. Thus PBHs (the mass and the energy fraction) act as a portal between gravitational waves and the parameters of high-energy particle physics models, motivating a synergic search of those models with GWs plus the conventional particle physics experiments. Such models featuring a high-scale gauged  $U(1)$ -symmetry breaking would exhibit the combined spectrum discussed in this article. See, e.g., recent work on the seesaw mechanism with a gauged  $U(1)$  symmetry [26], where the motivation and consequences of PBH domination have been studied. Studying this framework in the context of global strings, which generically appear in QCD-axion (including axionlike particles) models, might be interesting to explore in future works.

Before concluding, let us stress that the motivation of this paper is to point out that the consequences of an EMD due to the standard long-lived fields or some additional new physics and PBHs could be vastly different. In particular, distorting GWs spectrum from cosmic strings with EMD, results in a scale-invariant spectrum followed by a red tilt in both cases, while for the latter one, depending on the initial energy fraction of PBHs, a sharp blue tilt might follow or precede. This makes the PBH scenarios unique. More interestingly, depending on the model parameters, the new features ( $f_{\Delta}$  and  $f_{\text{peak}}$ ) in the scale-invariant spectrum might appear in a single detector (cf. Fig. 3). Additionally, because the effects of ultralight PBHs are of great interest to study, e.g., in the context of dark matter production, baryogenesis, and axions, such spectral features in the GWs could be a unique probe of these models, irrespective of the particle physics coupling strength. Let us also mention another interesting aspect of the PBH-string scenario. We focus on the frequency range where dominant GWs come from the post-PBH evaporation era, i.e., from the beginning of the most recent radiation domination. Although we do not discuss the detailed spectral shapes of the high-frequency GWs that might arise from the loops produced during PBH domination and before, an additional effect might be at play, distorting the high-frequency part of the spectrum. This effect is black hole–string interaction which has been studied analytically in the context of long-lived black holes, contributing to the dark matter density [114]. The average separation of PBHs after formation is  $d \simeq \lambda^{-1/3} t_f$ , where  $\lambda \ll 1$  is the fraction of horizon that turns into PBHs. In this case, long strings of average length  $l \simeq t_f/\lambda$  and interaction probability  $\lambda$  [114] connecting two

BHs can randomly chop off loops less than the size of the horizon ( $\alpha \simeq 0.1$ )  $t \sim t_f$ . Therefore, the string dynamics are largely unaffected by the PBH during the initial stages of evolution after PBH formation, and the usual computation of GWs from cosmic string loops holds. Nonetheless, the efficiency of chopping off loops of horizon size or less reduces as time evolves when the PBH separation connecting long strings become comparable to the horizon, and two PBHs tend to straighten long strings. The exact quantification of such a phenomenon requires appropriate numerical simulation.

## V. CONCLUSION

We have proposed a unique gravitational wave-based probe of superhigh scale  $U(1)$  symmetry breaking with a PBH-dominated epoch before the BBN era. While cosmic strings resulting from  $U(1)$  breaking lead to a typical scale-invariant GW spectrum, ultralight PBH domination leads to an additional observable GW spectrum from density fluctuations. When combined, the GW spectrum has a unique shape with a plateau, a sharp tilted peak, and a characteristic falloff behavior. Depending on the cosmic string and the PBH parameters, different parts of the spectrum fall within reach of ongoing and planned future experiments. While early matter domination, e.g., by a scalar field or supercooled first-order phase transition along super-high scale  $U(1)$  symmetry breaking can lead to a flat plateau followed by a falloff, peak over a flat plateau or combination of both, it remains distinguishable from the spectrum we obtain in the presence of PBHs. This is due to the lower and upper bounds on peak frequency in our work due to the allowed ultralight PBH mass window, which does not exist in other scenarios, plus the distinct power-law behavior of the GWs from PBH density fluctuations. In addition to such marked features verifiable in GW detectors, the setup discussed in our work can also have very rich phenomenological implications connected to the production of dark matter from PBH evaporation, high-scale leptogenesis, and seesaw for neutrino mass related to  $U(1)$  symmetry breaking [20,21,24–26].

## ACKNOWLEDGMENTS

The work of D.B. is supported by Science and Engineering Research Board (SERB), Government of India Grant No. MTR/2022/000575. R.S. acknowledges the European Structural and Investment Funds and the Czech Ministry of Education, Youth and Sports (Project CoGraDS No. CZ.02.1.01/0.0/0.0/15003/0000437) for the financial support. R.R. acknowledges the National Research Foundation of Korea (NRF) grant funded by the Korean government (No. 2022R1A5A1030700) and also the support provided by the Department of Physics, Kyungpook National University.

- [1] B. P. Abbott *et al.* (LIGO Scientific and Virgo Collaborations), Observation of Gravitational Waves from a Binary Black Hole Merger, *Phys. Rev. Lett.* **116**, 061102 (2016).
- [2] R. Caldwell *et al.*, Detection of early-universe gravitational-wave signatures and fundamental physics, *Gen. Relativ. Gravit.* **54**, 156 (2022).
- [3] A. Vilenkin, Cosmic strings and domain walls, *Phys. Rep.* **121**, 263 (1985).
- [4] P. Langacker, The physics of heavy  $Z'$  gauge bosons, *Rev. Mod. Phys.* **81**, 1199 (2009).
- [5] T. W. B. Kibble, Topology of cosmic domains and strings, *J. Phys. A* **9**, 1387 (1976).
- [6] H. B. Nielsen and P. Olesen, Vortex line models for dual strings, *Nucl. Phys.* **B61**, 45 (1973).
- [7] A. Vilenkin, Gravitational radiation from cosmic strings, *Phys. Lett.* **107B**, 47 (1981).
- [8] N. Turok, Grand unified strings and galaxy formation, *Nucl. Phys.* **242B**, 520 (1984).
- [9] Z. Arzoumanian *et al.* (NANOGrav Collaboration), The NANOGrav 12.5 yr data set: Search for an isotropic stochastic gravitational-wave background, *Astrophys. J. Lett.* **905**, L34 (2020).
- [10] B. Goncharov *et al.*, On the evidence for a common-spectrum process in the search for the nanohertz gravitational-wave background with the Parkes pulsar timing array, *Astrophys. J. Lett.* **917**, L19 (2021).
- [11] J. Ellis and M. Lewicki, Cosmic String Interpretation of NANOGrav Pulsar Timing Data, *Phys. Rev. Lett.* **126**, 041304 (2021).
- [12] S. Blasi, V. Brdar, and K. Schmitz, Has NANOGrav Found First Evidence for Cosmic Strings?, *Phys. Rev. Lett.* **126**, 041305 (2021).
- [13] R. Samanta and S. Datta, Gravitational wave complementarity and impact of NANOGrav data on gravitational leptogenesis, *J. High Energy Phys.* **05** (2021) 211.
- [14] M. Hindmarsh and J. Kume, Multi-messenger constraints on Abelian-Higgs cosmic string networks, *J. Cosmol. Astropart. Phys.* **04** (2023) 045.
- [15] Y. Cui, M. Lewicki, D. E. Morrissey, and J. D. Wells, Cosmic archaeology with gravitational waves from cosmic strings, *Phys. Rev. D* **97**, 123505 (2018).
- [16] Y. Cui, M. Lewicki, D. E. Morrissey, and J. D. Wells, Probing the pre-BBN universe with gravitational waves from cosmic strings, *J. High Energy Phys.* **01** (2019) 081.
- [17] Y. Gouttenoire, G. Servant, and P. Simakachorn, Beyond the standard models with cosmic strings, *J. Cosmol. Astropart. Phys.* **07** (2020) 032.
- [18] R. Allahverdi and J. K. Osiński, Early matter domination from long-lived particles in the visible sector, *Phys. Rev. D* **105**, 023502 (2022).
- [19] D. Borah, S. Jyoti Das, A. K. Saha, and R. Samanta, Probing WIMP dark matter via gravitational waves' spectral shapes, *Phys. Rev. D* **106**, L011701 (2022).
- [20] B. Barman, D. Borah, S. Das Jyoti, and R. Roshan, Cogenesis of baryon asymmetry and gravitational dark matter from PBH, *J. Cosmol. Astropart. Phys.* **08** (2022) 068.
- [21] D. Borah, S. Jyoti Das, and R. Roshan, Probing high scale seesaw and PBH generated dark matter via gravitational waves with multiple tilts, [arXiv:2208.04965](https://arxiv.org/abs/2208.04965).
- [22] R. Zhou and L. Bian, Gravitational waves from cosmic strings after a first-order phase transition, *Chin. Phys. C* **46**, 043104 (2022).
- [23] F. Ferrer, A. Ghoshal, and M. Lewicki, Imprints of a supercooled universe in the gravitational wave spectrum from a cosmic string network, [arXiv:2304.02636](https://arxiv.org/abs/2304.02636).
- [24] S. Datta, A. Ghosal, and R. Samanta, Baryogenesis from ultralight primordial black holes and strong gravitational waves from cosmic strings, *J. Cosmol. Astropart. Phys.* **08** (2021) 021.
- [25] R. Samanta and F. R. Urban, Testing super heavy dark matter from primordial black holes with gravitational waves, *J. Cosmol. Astropart. Phys.* **06** (2022) 017.
- [26] D. Borah, S. Jyoti Das, R. Samanta, and F. R. Urban, PBH-infused seesaw origin of matter and unique gravitational waves, *J. High Energy Phys.* **03** (2023) 127.
- [27] A. Ghoshal, Y. Gouttenoire, L. Heurtier, and P. Simakachorn, Primordial black hole archaeology with gravitational waves from cosmic strings, [arXiv:2304.04793](https://arxiv.org/abs/2304.04793).
- [28] B. Carr, K. Kohri, Y. Sendouda, and J. Yokoyama, Constraints on primordial black holes, *Rep. Prog. Phys.* **84**, 116902 (2021).
- [29] K. Inomata, K. Kohri, T. Nakama, and T. Terada, Enhancement of gravitational waves induced by scalar perturbations due to a sudden transition from an early matter era to the radiation era, *Phys. Rev. D* **100**, 043532 (2019).
- [30] T. Papanikolaou, V. Vennin, and D. Langlois, Gravitational waves from a universe filled with primordial black holes, *J. Cosmol. Astropart. Phys.* **03** (2021) 053.
- [31] G. Domènech, V. Takhistov, and M. Sasaki, Exploring evaporating primordial black holes with gravitational waves, *Phys. Lett. B* **823**, 136722 (2021).
- [32] G. Domènech, C. Lin, and M. Sasaki, Gravitational wave constraints on the primordial black hole dominated early universe, *J. Cosmol. Astropart. Phys.* **04** (2021) 062; *J. Cosmol. Astropart. Phys.* **11** (2021) E01.
- [33] G. Domènech, Scalar induced gravitational waves review, *Universe* **7**, 398 (2021).
- [34] S. Blasi, V. Brdar, and K. Schmitz, Fingerprint of low-scale leptogenesis in the primordial gravitational-wave spectrum, *Phys. Rev. Res.* **2**, 043321 (2020).
- [35] S. Datta and R. Samanta, Gravitational waves-tomography of low-scale-leptogenesis, *J. High Energy Phys.* **11** (2022) 159.
- [36] C. Ringeval, M. Sakellariadou, and F. Bouchet, Cosmological evolution of cosmic string loops, *J. Cosmol. Astropart. Phys.* **02** (2007) 023.
- [37] J. J. Blanco-Pillado, K. D. Olum, and B. Shlaer, Large parallel cosmic string simulations: New results on loop production, *Phys. Rev. D* **83**, 083514 (2011).
- [38] W. Buchmüller, V. Domcke, K. Kamada, and K. Schmitz, The gravitational wave spectrum from cosmological  $B - L$  breaking, *J. Cosmol. Astropart. Phys.* **10** (2013) 003.
- [39] J. A. Dror, T. Hiramatsu, K. Kohri, H. Murayama, and G. White, Testing the Seesaw Mechanism and Leptogenesis with Gravitational Waves, *Phys. Rev. Lett.* **124**, 041804 (2020).
- [40] W. Buchmüller, V. Domcke, H. Murayama, and K. Schmitz, Probing the scale of grand unification with gravitational waves, *Phys. Lett. B* **809**, 135764 (2020).

- [41] S. F. King, S. Pascoli, J. Turner, and Y.-L. Zhou, Gravitational Waves and Proton Decay: Complementary Windows into Grand Unified Theories, *Phys. Rev. Lett.* **126**, 021802 (2021).
- [42] B. Fornal and B. Shams Es Haghi, Baryon and lepton number violation from gravitational waves, *Phys. Rev. D* **102**, 115037 (2020).
- [43] W. Buchmuller, V. Domcke, and K. Schmitz, Stochastic gravitational-wave background from metastable cosmic strings, *J. Cosmol. Astropart. Phys.* **12** (2021) 006.
- [44] G. S. F. Guedes, P. P. Avelino, and L. Sousa, Signature of inflation in the stochastic gravitational wave background generated by cosmic string networks, *Phys. Rev. D* **98**, 123505 (2018).
- [45] L. Sousa, P. P. Avelino, and G. S. F. Guedes, Full analytical approximation to the stochastic gravitational wave background generated by cosmic string networks, *Phys. Rev. D* **101**, 103508 (2020).
- [46] M. A. Masoud, M. U. Rehman, and Q. Shafi, Sneutrino tribrid inflation, metastable cosmic strings and gravitational waves, *J. Cosmol. Astropart. Phys.* **11** (2021) 022.
- [47] G. Lazarides, R. Maji, and Q. Shafi, Cosmic strings, inflation, and gravity waves, *Phys. Rev. D* **104**, 095004 (2021).
- [48] A. Afzal, W. Ahmed, M. U. Rehman, and Q. Shafi,  $\mu$ -hybrid inflation, gravitino dark matter and stochastic gravitational wave background from cosmic strings, *Phys. Rev. D* **105**, 103539 (2022).
- [49] G. Lazarides, R. Maji, and Q. Shafi, Gravitational waves from quasi-stable strings, *J. Cosmol. Astropart. Phys.* **08** (2022) 042.
- [50] G. Lazarides, R. Maji, R. Roshan, and Q. Shafi, Heavier  $W$ -boson, dark matter and gravitational waves from strings in an  $SO(10)$  axion model, *Phys. Rev. D* **106**, 055009 (2022).
- [51] R. Maji and Q. Shafi, Monopoles, strings and gravitational waves in non-minimal inflation, *J. Cosmol. Astropart. Phys.* **03** (2023) 007.
- [52] A. Vilenkin, Cosmic string dynamics with friction, *Phys. Rev. D* **43**, 1060 (1991).
- [53] D. P. Bennett and F. R. Bouchet, Evidence for a Scaling Solution in Cosmic String Evolution, *Phys. Rev. Lett.* **60**, 257 (1988).
- [54] D. P. Bennett and F. R. Bouchet, Cosmic String Evolution, *Phys. Rev. Lett.* **63**, 2776 (1989).
- [55] T. Vachaspati and A. Vilenkin, Gravitational radiation from cosmic strings, *Phys. Rev. D* **31**, 3052 (1985).
- [56] J. J. Blanco-Pillado, K. D. Olum, and B. Shlaer, The number of cosmic string loops, *Phys. Rev. D* **89**, 023512 (2014).
- [57] C. J. A. P. Martins and E. P. S. Shellard, Quantitative string evolution, *Phys. Rev. D* **54**, 2535 (1996).
- [58] C. J. A. P. Martins and E. P. S. Shellard, Extending the velocity dependent one scale string evolution model, *Phys. Rev. D* **65**, 043514 (2002).
- [59] L. Sousa and P. P. Avelino, Stochastic gravitational wave background generated by cosmic string networks: Velocity-dependent one-scale model versus scale-invariant evolution, *Phys. Rev. D* **88**, 023516 (2013).
- [60] P. Auclair *et al.*, Probing the gravitational wave background from cosmic strings with LISA, *J. Cosmol. Astropart. Phys.* **04** (2020) 034.
- [61] J. J. Blanco-Pillado, K. D. Olum, and B. Shlaer, Cosmic string loop shapes, *Phys. Rev. D* **92**, 063528 (2015).
- [62] J. M. Wachter and K. D. Olum, Gravitational Smoothing of Kinks on Cosmic String Loops, *Phys. Rev. Lett.* **118**, 051301 (2017); *Phys. Rev. Lett.* **121**, 149901(E) (2018).
- [63] J. M. Wachter and K. D. Olum, Gravitational backreaction on piecewise linear cosmic string loops, *Phys. Rev. D* **95**, 023519 (2017).
- [64] D. Matsunami, L. Pogosian, A. Saurabh, and T. Vachaspati, Decay of Cosmic String Loops Due to Particle Radiation, *Phys. Rev. Lett.* **122**, 201301 (2019).
- [65] P. Auclair, D. A. Steer, and T. Vachaspati, Particle emission and gravitational radiation from cosmic strings: Observational constraints, *Phys. Rev. D* **101**, 083511 (2020).
- [66] J. J. Blanco-Pillado and K. D. Olum, Stochastic gravitational wave background from smoothed cosmic string loops, *Phys. Rev. D* **96**, 104046 (2017).
- [67] T. Charnock, A. Avgoustidis, E. J. Copeland, and A. Moss, CMB constraints on cosmic strings and superstrings, *Phys. Rev. D* **93**, 123503 (2016).
- [68] S. W. Hawking, Black hole explosions, *Nature (London)* **248**, 30 (1974).
- [69] S. W. Hawking, Particle creation by black holes, *Commun. Math. Phys.* **43**, 199 (1975); *Commun. Math. Phys.* **46**, 206(E) (1976).
- [70] G. F. Chapline, Cosmological effects of primordial black holes, *Nature (London)* **253**, 251 (1975).
- [71] B. J. Carr, Some cosmological consequences of primordial black-hole evaporations, *Astrophys. J.* **206**, 8 (1976).
- [72] S. Hawking, Gravitationally collapsed objects of very low mass, *Mon. Not. R. Astron. Soc.* **152**, 75 (1971).
- [73] B. J. Carr and S. W. Hawking, Black holes in the early Universe, *Mon. Not. R. Astron. Soc.* **168**, 399 (1974).
- [74] S. Wang, T. Terada, and K. Kohri, Prospective constraints on the primordial black hole abundance from the stochastic gravitational-wave backgrounds produced by coalescing events and curvature perturbations, *Phys. Rev. D* **99**, 103531 (2019); *Phys. Rev. D* **101**, 069901(E) (2020).
- [75] C. T. Byrnes and P. S. Cole, Lecture notes on inflation and primordial black holes, [arXiv:2112.05716](https://arxiv.org/abs/2112.05716).
- [76] M. Braglia, A. Linde, R. Kallosh, and F. Finelli, Hybrid  $\alpha$ -attractors, primordial black holes and gravitational wave backgrounds, *J. Cosmol. Astropart. Phys.* **04** (2023) 033.
- [77] M. Crawford and D. N. Schramm, Spontaneous generation of density perturbations in the early universe, *Nature (London)* **298**, 538 (1982).
- [78] S. W. Hawking, I. G. Moss, and J. M. Stewart, Bubble collisions in the very early universe, *Phys. Rev. D* **26**, 2681 (1982).
- [79] I. G. Moss, Singularity formation from colliding bubbles, *Phys. Rev. D* **50**, 676 (1994).
- [80] H. Kodama, M. Sasaki, and K. Sato, Abundance of primordial holes produced by cosmological first order phase transition, *Prog. Theor. Phys.* **68**, 1979 (1982).
- [81] M. J. Baker, M. Breitbach, J. Kopp, and L. Mitnacht, Primordial black holes from first-order cosmological phase transitions, [arXiv:2105.07481](https://arxiv.org/abs/2105.07481).

- [82] K. Kawana and K.-P. Xie, Primordial black holes from a cosmic phase transition: The collapse of Fermi-balls, *Phys. Lett. B* **824**, 136791 (2022).
- [83] P. Huang and K.-P. Xie, Primordial black holes from an electroweak phase transition, *Phys. Rev. D* **105**, 115033 (2022).
- [84] K. Hashino, S. Kanemura, and T. Takahashi, Primordial black holes as a probe of strongly first-order electroweak phase transition, *Phys. Lett. B* **833**, 137261 (2022).
- [85] J. Liu, L. Bian, R.-G. Cai, Z.-K. Guo, and S.-J. Wang, Primordial black hole production during first-order phase transitions, *Phys. Rev. D* **105**, L021303 (2022).
- [86] S. W. Hawking, Black holes from cosmic strings, *Phys. Lett. B* **231**, 237 (1989).
- [87] H. Deng, J. Garriga, and A. Vilenkin, Primordial black hole and wormhole formation by domain walls, *J. Cosmol. Astropart. Phys.* **04** (2017) 050.
- [88] I. Masina, Dark matter and dark radiation from evaporating primordial black holes, *Eur. Phys. J. Plus* **135**, 552 (2020).
- [89] R. Anantua, R. Easther, and J. T. Giblin, GUT-Scale Primordial Black Holes: Consequences and Constraints, *Phys. Rev. Lett.* **103**, 111303 (2009).
- [90] J. L. Zagorac, R. Easther, and N. Padmanabhan, GUT-scale primordial black holes: Mergers and gravitational waves, *J. Cosmol. Astropart. Phys.* **06** (2019) 052.
- [91] R. Saito and J. Yokoyama, Gravitational Wave Background as a Probe of the Primordial Black Hole Abundance, *Phys. Rev. Lett.* **102**, 161101 (2009); *Phys. Rev. Lett.* **107**, 069901(E) (2011).
- [92] K. Inomata, M. Kawasaki, K. Mukaida, T. Terada, and T. T. Yanagida, Gravitational wave production right after a primordial black hole evaporation, *Phys. Rev. D* **101**, 123533 (2020).
- [93] B. Barman, D. Borah, S. Jyoti Das, and R. Roshan, Gravitational wave signatures of PBH-generated baryon-dark matter coincidence, *Phys. Rev. D* **107**, 095002 (2023).
- [94] T. Papanikolaou, Gravitational waves induced from primordial black hole fluctuations: The effect of an extended mass function, *J. Cosmol. Astropart. Phys.* **10** (2022) 089.
- [95] J. Kozaczuk, T. Lin, and E. Villarama, Signals of primordial black holes at gravitational wave interferometers, *Phys. Rev. D* **105**, 123023 (2022).
- [96] S. Blasi, V. Brdar, and K. Schmitz, Fingerprint of low-scale leptogenesis in the primordial gravitational-wave spectrum, *Phys. Rev. Res.* **2**, 043321 (2020).
- [97] Y. Gouttenoire, G. Servant, and P. Simakachorn, BSM with cosmic strings: Heavy, up to EeV mass, unstable particles, *J. Cosmol. Astropart. Phys.* **07** (2020) 016.
- [98] A. Weltman *et al.*, Fundamental physics with the Square Kilometre Array, *Publ. Astron. Soc. Aust.* **37**, e002 (2020).
- [99] J. Garcia-Bellido, H. Murayama, and G. White, Exploring the early universe with Gaia and THEIA, *J. Cosmol. Astropart. Phys.* **12** (2021) 023.
- [100] M. Kramer and D. J. Champion, The European pulsar timing array and the large European array for pulsars, *Classical Quantum Gravity* **30**, 224009 (2013).
- [101] A. Sesana *et al.*, Unveiling the gravitational universe at  $\mu$ -Hz frequencies, *Exp. Astron.* **51**, 1333 (2021).
- [102] P. Amaro-Seoane *et al.* (LISA Collaboration), Laser interferometer space antenna, arXiv:1702.00786.
- [103] S. Kawamura *et al.*, The Japanese space gravitational wave antenna DECIGO, *Classical Quantum Gravity* **23**, S125 (2006).
- [104] K. Yagi and N. Seto, Detector configuration of DECIGO/BBO and identification of cosmological neutron-star binaries, *Phys. Rev. D* **83**, 044011 (2011); *Phys. Rev. D* **95**, 109901(E) (2017).
- [105] M. Punturo *et al.* (ET Collaboration Collaboration), The Einstein Telescope: A third-generation gravitational wave observatory, *Classical Quantum Gravity* **27**, 194002 (2010).
- [106] B. P. Abbott *et al.* (LIGO Scientific Collaboration), Exploring the sensitivity of next generation gravitational wave detectors, *Classical Quantum Gravity* **34**, 044001 (2017).
- [107] J. Aasi *et al.* (LIGO Scientific Collaboration), Advanced LIGO, *Classical Quantum Gravity* **32**, 074001 (2015).
- [108] T. Fujita, M. Kawasaki, K. Harigaya, and R. Matsuda, Baryon asymmetry, dark matter, and density perturbation from primordial black holes, *Phys. Rev. D* **89**, 103501 (2014).
- [109] O. Lennon, J. March-Russell, R. Petrossian-Byrne, and H. Tillim, Black hole genesis of dark matter, *J. Cosmol. Astropart. Phys.* **04** (2018) 009.
- [110] G. Domènech and M. Sasaki, Gravitational wave hints black hole remnants as dark matter, arXiv:2303.07661.
- [111] G. Franciolini and P. Pani, Stochastic gravitational-wave background at 3G detectors as a smoking gun for microscopic dark matter relics, arXiv:2304.13576.
- [112] P. Gondolo, P. Sandick, and B. Shams Es Haghi, Effects of primordial black holes on dark matter models, *Phys. Rev. D* **102**, 095018 (2020).
- [113] N. Bernal, F. Hajkarim, and Y. Xu, Axion dark matter in the time of primordial black holes, *Phys. Rev. D* **104**, 075007 (2021).
- [114] A. Vilenkin, Y. Levin, and A. Gruzinov, Cosmic strings and primordial black holes, *J. Cosmol. Astropart. Phys.* **11** (2018) 008.